NREL/CP-520-25682

Effects of Substrate and Na Concentration on Device Properties, Junction Formation, and Film Microstructure in $CuInSe_2$ PV Devices

R.J. Matson, J.E. Granata, S.E. Asher, and M.R. Young
National Renewable Energy Laboratory

Presented at the National Center for Photovoltaics Program Review Meeting
Denver, Colorado
September 8-11, 1998

National Renewable Energy Laboratory
1617 Cole Boulevard
Golden, Colorado 80401-3393
A national laboratory of the U.S. Department of Energy
Managed by Midwest Research Institute
for the U.S. Department of Energy
under contract No. DE-AC36-83CH10093

Work performed under task number PV903201

October 1998

NOTICE

Available to DOE and DOE contractors from:
Office of Scientific and Technical Information (OSTI)
P.O. Box 62
Oak Ridge, TN 37831
Prices available by calling 423-576-8401

Available to the public from:
National Technical Information Service (NTIS)
U.S. Department of Commerce
5285 Port Royal Road
Springfield, VA 22161
703-605-6000 or 800-553-6847
or
DOE Information Bridge
http://www.doe.gov/bridge/home.html

Printed on paper containing at least 50% wastepaper, including 10% postconsumer waste

Effects of Substrate and Na Concentration on Device Properties, Junction Formation, and Film Microstructure in $CuInSe_2$ PV Devices

R.J. Matson, J.E. Granata, S.E. Asher, and M.R. Young

National Renewable Energy Laboratory, 1617 Cole Blvd., Golden, CO 80401, USA

Abstract. Different concentrations of Na were systematically introduced into $CuInSe_2$ (CIS) photovoltaic solar cell absorber material on different substrates (SLG, $Si0_2$/SLG, 7059, alumina) to: 1) determine the resultant effects on device properties, junction formation, and material microstructure; and 2) determine the optimal range of Na concentrations in the CIS films per specific substrate. In general, finished devices show improved V_{oc}, J_{sc}, and device efficiency, improved charge-collection efficiency and, possibly, increased grain size as a result of the coevaportion of 4 to 100 mg of Na_2Se during film deposition. However, a dramatic devolution set in with the addition of 235 mg of Na_2Se, and all the aforementioned parameters were either at, or worse than, their pre-Na-addition levels. Meanwhile, although the device microstructure improves with Na addition and, more importantly, the junction (as characterized by electron-beam-induced current) has become much more uniform and closer to the heteroface, all that reverses with the "Na overdose."

INTRODUCTION

Along with others, we have observed that the substrate and the back contact affect the performance of CIS photovoltaic solar cells, and that soda-lime glass (SLG) is the preferred substrate for highly efficient CIS-based devices. These combined observations suggest that the primary reason for the performance improvements is the indiffusion of impurities from the glass (potassium, calcium, and, in particular, sodium) through the back contact and into the absorber. Although the improvements in morphology and device characteristics with the presence of Na have been noted by others, most data to date are qualitative regarding actual Na content. Building on recent results (1,2), we attempt to quantitatively demonstrate the range of Na concentration in the absorber necessary for four different substrates for optimal device performance, and to correlate this range with film microstructure, junction formation, and device properties. In this study, alumina, 7059 glass, and $Si0_2$/SLG were also studied as contrasts and logical alternatives to the more common SLG case.

EXPERIMENT

Devices were fabricated on four different substrates: namely, SLG/Mo, SLG/$Si0_2$/Mo (where the $Si0_2$ was intended to attenuate the Na indiffusion from the SLG), alumina/Mo,

and 7059 glass (a.k.a. borosilicate glass or BSG, to test cases where there is naturally very little Na indiffusion). CIS absorbers were then deposited on the Mo for each substrate using a standard three-stage, physical-vapor-deposition process. Sodium was introduced in the form of Na_2Se and was coevaporated with Cu and Se during the second stage of the absorber deposition. Six CIS depositions were performed using six different quantities of Na_2Se during deposition, namely 0, 4, 8, 40, 100, and 235 mg. Following the absorber deposition, a 50-nm layer of chemical-bath-deposited CdS was deposited and the devices were finished with a bilayer of radio-frequency-sputtered ZnO. A Ni-Al grid completed device processing.

Absorber layers were then analyzed using inductively coupled plasma (ICP) spectroscopy, secondary ion mass spectrometry (SIMS), and scanning electron microscopy (SEM). The finished solar cells were characterized by current voltage, capacitance voltage, and electron-beam-induced current (EBIC) measurements. The specifics of the Na concentration measurements are given elsewhere (1).

DATA AND RESULTS

In the earlier work, and not unexpectedly, where there was an intercomparison of the effect of varying Na concentrations in CIS on just SLG/Mo substrates, but from three different manufacturers, the overall trends in performance versus Na concentration were more consistent (1). In this experimental matrix, the varied substrates further complicate comparison and analysis. The 7059 case is additionally problematic in that the processing itself was not optimized and the substrate temperatures were possibly too high, which resulted in film peeling in the 235-mg case and precluded any device-related measurements.

Device Characterization. The intercomparison of the amount of Na_2Se added during processing, the corresponding SIMS-measured Na concentrations in atomic percent, the junction depletion width (W [um]), V_{oc} (mV), J_{sc} (mA/cm^2), and device efficiency (%) are presented in Table 1. The Na dosage is noted in terms of the 0, 4, 8, 40, 100, or 235 mg of the Na_2Se coevaporated during the device deposition on the four different substrates. In viewing the array of Na concentrations, one can roughly distinguish three main categories: no Na added (0 mg), a low-to-moderate amount of Na added (4–100 mg), and a high or toxic amount of Na added (the 235-mg case). Regarding the SIMS results, note that: 1) only factors of two or greater in concentrations can begin to be taken as significant; 2) the variations in measured concentrations seen in the 0–100 mg cases still remain somewhat ambivalent in terms of their absolute quantitative significance, but should be useful for purposes of general intercomparison; 3) the SIMS sampling area is on the order of 60μm; and 4) the SIMS were not reproducible everywhere on a given sample, so the lowest Na level was used. Further, the devices themselves are not record devices.

Table 1. Na concentration (atomic percent times 10^{+3} for ease of comparison), depletion width [W(μm)], V_{oc} (mV), J_{sc} (mA/cm^2), and efficiency (%) as a function of the four different device substrates and six different amounts of Na_2Se [mg] added during deposition.

Additional Na_2Se [mg]	At. %. ($x10^{+3}$)	W [μm]	V_{oc} [mV]	J_{sc}[mA/ cm^2]	Eff. [%]
		Alumina substrate			
0	0.04	0.8	0.33	32.0	6.4
4	0.08	0.5	0.36	34.5	6.4
8	0.06	0.7	0.38	33.5	8.1
40	0.2	0.5	0.37	31.0	6.6
100	0.2	0.7	0.33	35.0	6.8
235	300.	0.2	0.43	26.5	6.9
		7059 / BSG substrate			
0	0.06	0.9	0.34	30.5	5.5
4	0.05	0.5	0.42	32.4	7.0
8	0.08	1.1	0.41	20.4	3.3
40	0.2	0.4	0.39	32.3	8.3
100	0.5	0.8	0.39	27.8	4.9
235	300. NA	NA	NA	NA	
		SLG substrate			
0	20.	0.6	0.42	32.6	9.4
4	60.	0.4	0.44	34.9	10.6
8	80.	0.5	0.46	33.9	11.1
40	50.	0.5	0.44	33.3	10.6
100	40.	0.4	0.44	34.8	10.0
235	500.	0.2	0.42	28.7	7.1
		SiO_2 / SLG substrate			
0	0.06	1.0	0.33	33.1	6.6
4	0.2	0.5	0.31	34.1	5.8
8	0.5	0.8	0.31	33.2	5.9
40	3.	0.6	0.34	32.5	6.9
100	12.	0.8	0.29	28.0	4.3
235	400. 0.3	0.40	28.4	5.2	

Device Microcharacterization

Corresponding to the matrix of device properties in Table I, there is microcharacterization in the form of EBIC linescans (or charge-collection efficiency profiles) superimposed on secondary electron images of cross sections of the same devices in Figure 1. (See Ref. 3 for more details on the technique.) Note the device structure in each case, from left to right: the ~1.0-μm-thick Mo back contact, the 2–3-μm-thick CIS absorber layer, the ~0.3–0.4-μm-thick CdS/ZnO window layer, and also note the heteroface between the window layer and the absorber layer as the junction depth is measured with respect to this interface. Because the internal quantum efficiency (QE_{int}) can be determined by the convolution of the optical generation function and the charge-collection efficiency profile represented by the EBIC linescan, we should be able to anticipate both the QE_{int} and something about the J_{sc} from the EBIC linescan. One also expects the V_{oc} to be reflected in

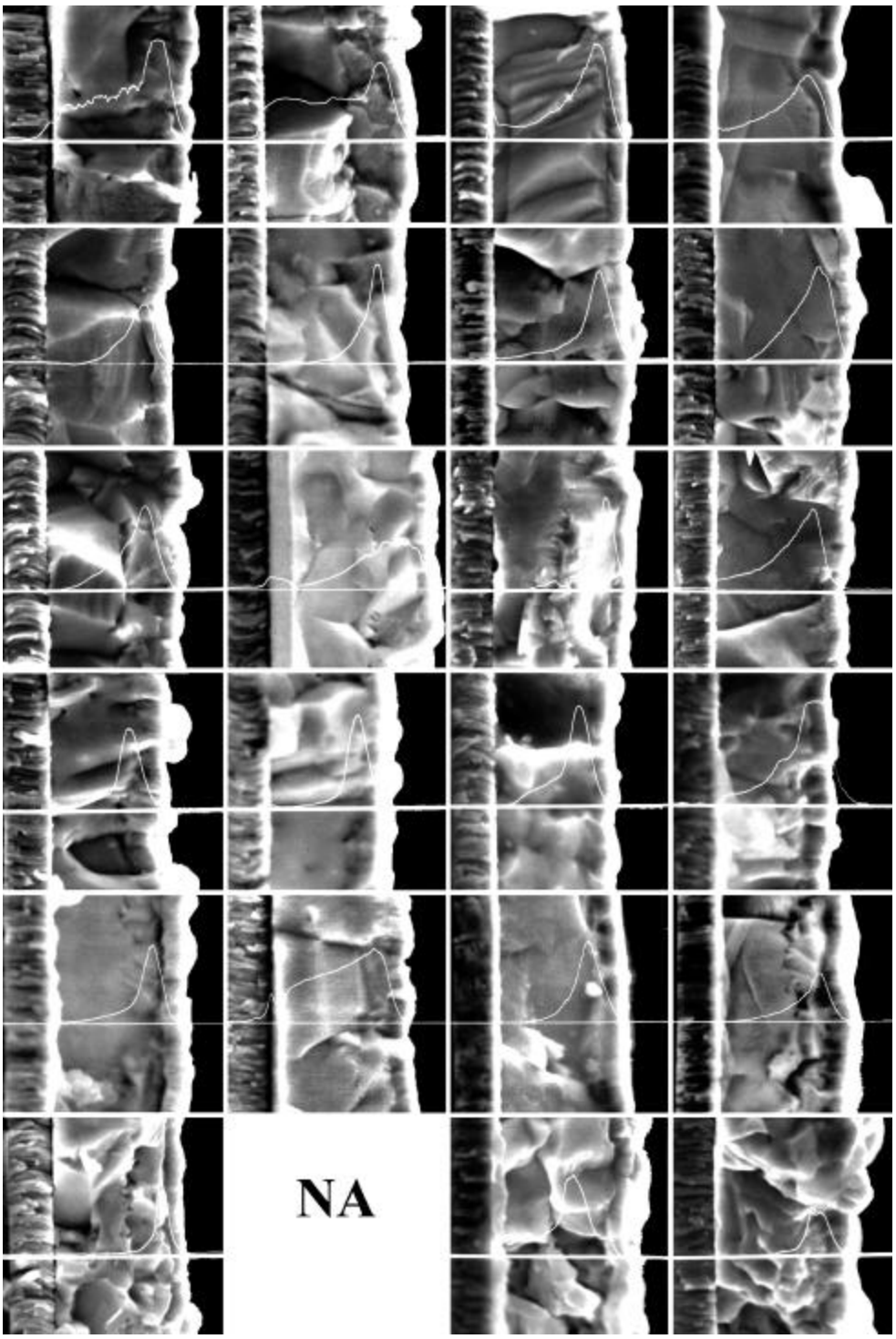

Figure 1. Single EBIC linescans on SEM micrographs of device cross sections for the different device conditions. To wit, the different substrates, from left to right: alumina, 7059, SLG, SiO_2/SLG. From top to bottom, the Na concentrations: 0, 4, 8, 40, 100, 235 mg of coevaporated Na in each substrate category.

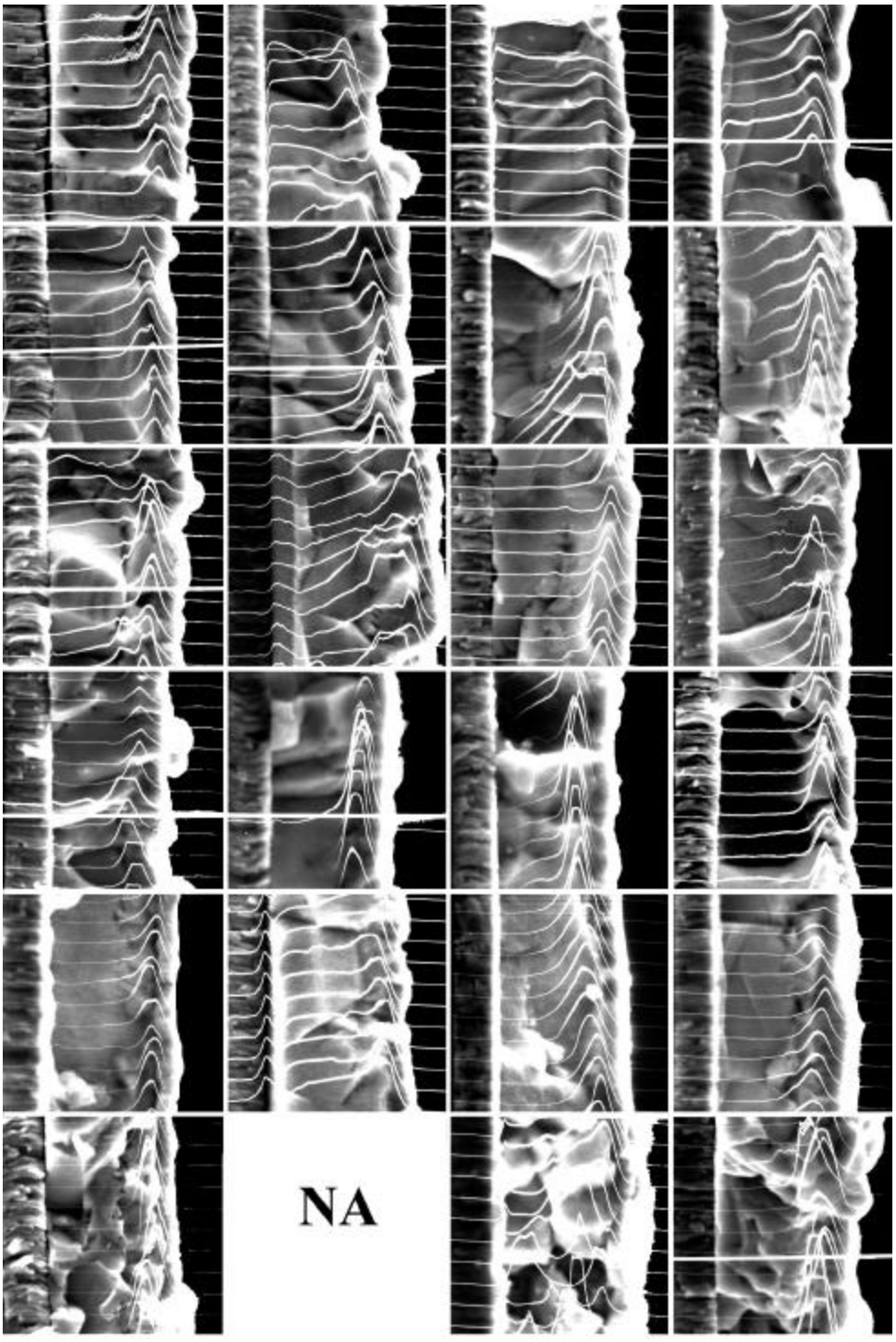

Figure 2. This series follows the progression in Figure 1, except in terms of multiple linescans on the device cross section tO demonstrate existing nonuniformity in electrical properties at the micron and submicron scale.

the abruptness of the junction and, therefore, the abruptness, or sharpness, of the EBIC peak—barring other mitigating factors. Because of the complexity of the defect chemistry and the resultant nonuniformity in the electrical properties of this material system on a local scale, often just one linescan cannot adequately represent a device. Hence, Figure 2 provides the same matrix of devices with the same general characterization format, except with multiple EBIC linescans to demonstrate the uniformity or nonuniformity of the particular category of device. Note that topography only has a secondary effect on the basic information contained in the EBIC profile. These figures also demonstrate the combined effects of the additional Na and the substrates on the topography or microstructure.

ANALYSIS AND DISCUSSION

Although less than straightforward, we can still denote certain useful trends in these material systems and devices. To wit:

1) The measurements of the Na concentrations were not affected in the systematic manner one might expect from the additional Na added during evaporation. They are to be taken as approximate and useful for intercomparisons. It would appear that possibly the substrate may largely determine the Na content up until the 235-mg case, where it has finally suffered a toxic overdose of Na. This is the point where both the device properties and the microstructure have devolved past the zero-Na addition case.

2) Generally speaking, the depletion width narrows and the V_{oc}, J_{sc}, and device efficiency improve with the first addition of Na, and then remains approximately constant within the 4–100-mg cases. With the Na overdose, or 235-mg case, the devices tend to degrade—more importantly, in the case of SLG. The effects of the additional Na on the individual parameters of the devices with differing substrates are not wholly consistent with one another. Overall, it can be said that: a) the SLG case mirrors the earlier work (1); b) the variations in the device efficiency and related parameters in the SLG/$Si0_2$ case defy immediate analysis; c) while the alumina case loses J_{sc} with the higher Na content, it gains in V_{oc} to maintain about the same efficiency; and d), and again anomolously, there is an initial improvement, then a degradation, then another improvement, and finally a significant degradation again by the 100-mg case with the 7059 substrate. The 235-mg film freely peeled off of the Mo/7059 substrate.

3) In terms of microcharacterization, despite the seemingly small addition of Na in the 4-mg case (as measured by SIMS), one sees the junction becoming significantly more "coherent," i.e., more uniform, narrower (a clear decrease in depletion width as confirmed by C-V measurements), and with the junction located closer to the heteroface. In moving from 4 to 8 mg, the EBIC profile and junction uniformity remains about the same, except in the 7059 case where it appears to revert to a much greater nonuniformity. From 8 to 40 mg, the junction moves forward slightly and the material becomes a bit more coherent again. From 40 to 100 mg, we have mixed results: where the alumina case narrows, the 7059 broadens and becomes nonuniform, and the SLG case is a bit ambiguous. From the 100–235 mg

case, where the junction depth and width decrease in the alumina case, they increased in the SLG cases. The 235-mg case for the 7059 substrate is not represented because the film peeled off and could not be measured.

One could argue, as others have (4,5), that the microstructure shows a possible overall tendency to improve through the midrange of Na values. The microstructure appears here, however, to simply disintegrate with the highest Na content. Unless the Na, or some other more complicated defect chemistry simultaneously served to passivate them, a corresponding increase in surface states and defects would be expected with this disintegration because of increased grain surfaces. Where some have reported an unambiguous increase in grain size or coherence of the film with increasing Na content (4) such an evolution is not so clear to us (Figures 1 and 2). Also, whatever increasing crystallinity (larger, tighter grain structure) there may be, it appears to occur from the top of the film down toward the substrate. However, it must be noted that any differences between our set of results and others could easily be attributed to any number of processing variables. What is clear, and corresponds well with the poor device properties, is that the whole microstructure breaks down into much smaller grained material throughout the film, and becomes quite porous with Na concentrations in the 0.3 to 0.5 at. % range.

CONCLUSIONS

From the device parameters and SEM microcharacterization, we offer a few observations: 1) the initial device performance values are substrate-dependent and are also ordered roughly according to the amount of Na present; 2) the V_{oc}, FF, and hole concentrations generally improve as Na is added up to incorporated concentrations on the order of less than a tenth of an atomic percent; 3) above ~0.1 at. %, all parameters change significantly including the microstructure and diode behavior; 4) the microstructure of the material and the charge-collection efficiency profiles provide additional clues concerning the evolution and devolution of the material/defect properties with Na incorporation; and 5) the ideal Na concentration range depends on the substrate, because there are varying degrees of "preloading," or indiffusion, of Na depending on substrate—most notably the SLG substrate.

In addition, and somewhat ambiguously, the EBIC profiles indicate increasing uniformity in the charge-collection efficiency depth profile with both narrower peaks in charge collection and peaks closer to the heteroface with increasing Na (which suggests both improved V_{oc} and short-wavelength response). With the specific and local changes in a quite complex defect chemistry being less than obvious, we noted a progression from a distinct nonuniform response, to a greater uniformity and a "gathering of the response," and, finally, to a relatively coherent or uniform EBIC response (that is, for this material system) closer to the heteroface. This is where one would expect optimal charge collection to occur. Then we note, in the higher Na range, that with just a relatively small addition of Na, the uniformity of the junction properties degrades a bit. Finally, by the 235-mg case or 0.3–0.5 at. % of Na incorporation, the material integrity and uniformity of EBIC response degrade dramatically.

Even in the alumina case where the EBIC uniformity remains intact, the electron-beam quantum efficiency, or device performance, degrades.

One possible partial explanation of these phenomena is that at high Na concentrations, a detrimental Na-containing compound is formed and acts as a secondary phase in the absorber. SIMS data show that the Na accumulates in the front of the film in CIS, even though it is added toward the back. This suggests that the main mode of Na transport is via grain boundaries, and that the Na that resides in the bulk is at a lower level. Hence, either this low level is enough to improve device performance or, as the history of the investigation of this material suggests, the electronic life of the material takes place primarily at the grain surfaces. That the improved device properties systematically correspond to increased uniformity of the microstructure of the material is still open to question; however, overall the device properties improved with additional Na—but only up to a point. With excessive Na, we observed a rapid degradation of device properties and dramatically decreased grain size and increased material porosity (and, therefore, increased grain surface area and possible number of defect sites) occurred. One could postulate that the increased V_{oc} is a consequence of a higher effective acceptor concentration in the absorber material caused by some direct or indirect passivation role by the Na which, in turn, results in a reduction of electrically active deep trap states at the grain surface. Then, with the formation of a possible second phase, we see a competing effect reversing the earlier gains. Clearly, additional work in this area is needed to explain these data, let alone provide the foundations for a complete phenomenological model for this complex electronic material.

ACKNOWLEDGEMENTS

The authors wish to thank A. Mason for help with EPMA; T. Berens, K. Ramanathan, J. Keane, J. Alleman, and J. Dolan for help with device fabrication; and NREL. This work was performed under U.S. Department of Energy Contract No. DE-AC36-83CH10093 and NREL subcontract XAX-4-14000-01.

REFERENCES

1. Granata, J.E., J.R. Sites, S. Asher, and R.J. Matson, "Quantitative incorporation of sodium in $CuInSe_2$ and $Cu(InGa)Se_2$ photovoltaic devices," *Proc. 26th IEEE PVSC, Anaheim2*, 1997, p. 387.

2. Granata, J.E. and J.R. Sites, "Impact of sodium in the bulk and in grain boundaries of $CuInSe_2$," *Proceedings of the Second World Conference on Photovoltaic Solar Energy Conversion, Vienna*, July, 1998. (In press.)

3. Matson, R.J., "Applications of charge collection microscopy/electron-beam-induced current to semiconductor material and device research*," Scanning Microscopy*, Supplement 7, 1993, p. 243.

4. Hedstrom, J., H. Ohlsen, M. Bodegard, A. Kylner, L. Stolt, D. Hariskos, M. Ruckh, and H.-W. Schock, "ZnO/CdS/$Cu(In,Ga)Se_2$ thin film solar cells with improved performance," *Proc. 23rd IEEE PVSC, Louisville*, 1993, p. 364.

5. Bodegard, M., J. Hedstrom, K. Granath, A. Rockett, and L. Stolt, "Na precursors for coevaporated $Cu(In,Ga)Se_2$ photovoltaic films," *Proc. 13th European Photovoltaic Solar Energy Conference*, 1995, p. 2080.